DOI: 10.1002/zaac.201500083

Synthesis, Crystal Structure, Optical, Magnetic and Thermal Properties of $(NH_4)_2Mn[B_2P_3O_{11}(OH)_2]Cl$

Katharina Förg[a] and Henning A. Höppe*[a]

Dedicated to Professor Rüdiger Kniep on the Occasion of His 70th Birthday

Keywords: Borophosphate; Chloride; Crystal structure; Manganese; Vibrational spectroscopy

Abstract. $(NH_4)_2Mn^{II}[B_2P_3O_{11}(OH)_2]Cl$ was synthesized as a crystalline colorless powder by reaction of $MnCl_2$, $(NH_4)_2HPO_4$, H_3BO_3, and H_3PO_4 under hydrothermal conditions at 180 °C. According to X-ray single-crystal investigations $(NH_4)_2Mn[B_2P_3O_{11}(OH)_2]Cl$ crystallizes in a new structure type in the monoclinic space group $P2_1/n$ (no. 14) [Z = 4, a = 905.24(3), b = 847.29(3), c = 1652.32(5) pm, β = 92.303(1)°, R_1 = 0.025, wR_2 = 0.063, 2227 data, 229 parameters]. The crystal structure comprises infinite layers of corner-sharing borate, hydroxo-borate phosphate, and hydroxo-phosphate tetrahedra with Mn^{2+}, NH_4^+, and Cl^- ions in-between. The loop-branched (lB) vierer-single layer reveals an open-branched (oB) vierer-single ring as a novel fundamental building unit (FBU) $^2_\infty[B_2P_3\Phi_{13}]$ (Φ = O, OH). The Mn atom is coordinated slightly distorted octahedrally by five oxygen atoms from two different borophosphate layers and one chlorine atom. Amongst others the magnetic properties of the compound are presented confirming that the compound obeys Curie's law.

Introduction

Since the resumption of research in borophosphates in the 1990s[1–10] this class of compounds exhibits a great variety in composition and structure; certainly we are aware of the fact that systematic nomenclature would name such compounds as "phosphatoborates" but since "borophosphates" is being used throughout the common literature we also use the latter. Borophosphates are isoelectronic to silicates[1,11,12] and are thus subject of investigations for promising properties. One structural feature – the B–O–P linkage – all borophosphates have in common. Until now no P–O–P linking has been observed. This avoidance appears analogously to alumosilicates, where according to Loewenstein's[13] as well as to Pauling's rule concerning the nature of contiguous polyhedra[14] Al–O–Al linkages of tetrahedra are rarely observed.[12] In borophosphates phosphorus adopts always the coordination $P\Phi_4$ (Φ = O, OH), while boron can be coordinated in a trigonal-planar $B\Phi_3$ or tetrahedral manner, i.e. $B\Phi_4$.[12] For classification of borophosphates anionic partial structures are fractionized into their so-called fundamental building units (FBUs), an assignment which is overtaken analogously from silicate and borate chemistry.[11,12,15,16] Comprising the essential structural motif, the FBU displays one characteristic feature of a respective borophosphate. Besides the B:P ratio the O:OH ratio plays an important role as well.

A number of compounds with a B:P ratio of 2:3 is well known. Depending on the O:OH ratio and the FBU the polymeric borophosphate anion forms chains or layers.[5,17–21]

Herein we represent the crystal structure of a new diammonium-manganese(II)borophosphate-chloride $(NH_4)_2Mn[B_2P_3O_{11}(OH)_2]Cl$ with a novel FBU as well as its optical, magnetic, and thermal properties.

Results and Discussion

Crystal Structure

$(NH_4)_2Mn[B_2P_3O_{11}(OH)_2]Cl$ (**I**) crystallizes in a new structure type in the monoclinic space group $P2_1/n$ (Table 1, Table 2, and Table 3). The anionic partial structure of **I** consists of infinite layers of corner-sharing borate, hydroxo-borate, phosphate and hydroxo-phosphate tetrahedra (Figure 1) avoid-

Table 1. Selected interatomic distances /pm and angles /° in $(NH_4)_2Mn[B_2P_3O_{11}(OH)_2]Cl$.[a)]

B–O_{br}	145.4(3)–148.1(3)
B–O_H	143.4(3)
P–O_{br}	152.73(16)–157.50(15)
P–O_{term}	149.03(16)–150.42(16)
P–O_H	155.60(17)
Mn–O	212.31(16)–227.74(16)
Mn–Cl	257.45(7)
B–O_{br}–P	127.58(14)–136.72(16)

a) O_{br} = bridging oxygen atom; O_{term} = terminal oxygen atom; O_H = oxygen atom of hydroxyl group.

* Prof. Dr. H. A. Höppe
Fax: +49-821-598-5955
E-Mail: henning@ak-hoeppe.de
[a] Institut für Physik
Universität Augsburg
Universitätsstr. 1
86159 Augsburg, Germany
Supporting information for this article is available on the WWW under **http://dx.doi.org/10.1002/zaac.201500083** or from the author.

ing any P–O–P connection. All atoms are located on general positions. The polyanion is constructed by cyclic pentameric $^{2}_{\infty}[B_2P_3\Phi_{13}]$ (Φ = O, OH) units comprising a B:P ratio of 2:3. The loop-branched (lB) vierer-single layer contains an open-branched (oB) vierer-single ring as a novel FBU formed by two $B\Phi_4$ (Φ = O, OH) and three $P\Phi_4$ (Φ = O, OH) tetrahedra, illustrated with the descriptor 5□:<4□>□. Till now protonated borophosphates with a B:P ratio of 2:3 are divided into anionic partial structures with oB dreier single-rings and open-loop-branched (olB) dreier single-rings. Whereas chain borophosphates can be either formed by olB or oB dreier single-rings with an O:OH ratio of 11:2 or 12:1, layer borophosphates are only formed with oB dreier single-rings and show an O:OH ratio of 12:1.[12]

Table 2. MAPLE calculations for $(NH_4)_2Mn[B_2P_3O_{11}(OH)_2]Cl$.[47–49]

$(NH_4)_2Mn[B_2P_3O_{11}(OH)_2]Cl$	MnO [27] + B_2O_3 [28] + NH_4Cl [29] + $NH_4H_2PO_4$ [30] + P_2O_5 [31]
MAPLE = 124335 kJ·mol^{-1} Δ = 0.7 %	MAPLE = 125167 kJ·mol^{-1}

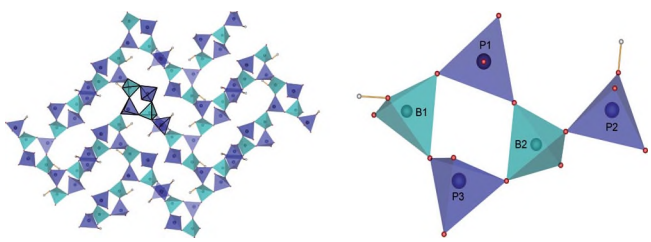

Figure 1. Layered anionic partial structure of $(NH_4)_2Mn[B_2P_3O_{11}(OH)_2]Cl$ exhibiting cyclic $^{2}_{\infty}[B_2P_3\Phi_{13}]$ (Φ = O, OH) units and the novel FBU as an oB vierer-single ring 5□:<4□>□ (phosphate tetrahedra blue, borate tetrahedra turquoise).

So far borophosphate compounds with an O:OH ratio of 11:2 never revealed a layered structure, but with $(NH_4)_2Mn[B_2P_3O_{11}(OH)_2]Cl$ we observed this structural feature for the first time. Moreover, in borophosphate chemistry no such FBU as the oB vierer-single ring $^{2}_{\infty}[B_2P_3\Phi_{13}]$ (Φ = O, OH) is known so far to our best knowledge. Both B and P atoms are coordinated tetrahedrally by either oxygen atoms or hydroxyl groups. B–O bond lengths in the borate tetrahedra range between 143 and 148 pm, whereas P–O bond lengths in the phosphate tetrahedra in **I** lie between 149 and 157 pm. The bond lengths B–O_H (boron attached to OH) and P–O_H are 143 pm and 156 pm, respectively. B–O_{br} (boron attached to bridging oxygen) distances range between 146 and 148 pm, whereas P–O_{br} distances range between 153 and 158 pm; P–O_{term} distances (phosphorus bound to terminal oxygen atoms) lie between 149 and 150 pm. These values correspond to typical data found for other borophosphates.[5,18,21,37] Selected bond lengths and angles of **I** are listed in Table 1.

An appropriate method for the calculation of deviation of tetrahedra from ideal symmetry was introduced by *Balić-Žunić* and *Makovicky*.[22,23] We adopted and explained this method on the example of α-$BaHPO_4$.[24] The five crystallographically different borate, hydroxo-borate, phosphate and hydroxo-phosphate tetrahedra in **I** feature the values –0.22 % (B1), –0.60 % (B2), –0.19 % (P1), –0.21 % (P2), and –0.46 % (P3) and are thus classified as regular, which holds for those polyhedra exhibiting a deviation below 1 %. The parallel borophosphate layers are interconnected via common oxygen corners of MnO_5Cl octahedra as demonstrated in Figure 2.

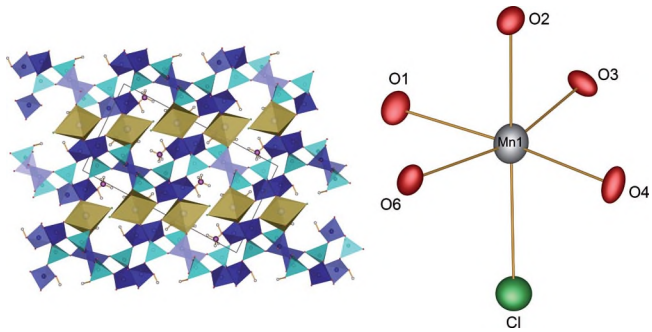

Figure 2. Layered crystal structure viewed along [010] interconnected via common O corners of MnO_5Cl octahedra (yellow) and coordination sphere of manganese in $(NH_4)_2Mn[B_2P_3O_{11}(OH)_2]Cl$, the displacement ellipsoids are drawn on a probability level of 65 %.

The single-crystal structure analysis reveals one unique site of the Mn^{2+} ion, which is coordinated distorted octahedrally by chlorine and five oxygen atoms (Figure 2). The coordinating oxygen atoms originate from a hydroxyl group of a borate and terminal oxygen atoms of four phosphate tetrahedra belonging to two adjacent borophosphate layers. The Mn–O bond lengths range between 212–228 pm, the Mn–Cl distance amounts to 257 pm (Table 1); these values are in excellent agreement with the sum of the ionic radii of *high-spin*-Mn^{II} and the coordinating atoms, i.e. 215 (OH), 218 (O) and 264 pm (Cl),[25] respectively.

Along [100] and [111] oval shaped channels (approx. 700 × 440 pm) are formed (Figure 3), in which the NH_4^+ ions are situated. According to *Steiner*[26] hydrogen bonds comprising donor-acceptor distances between 250 and 320 pm can be considered as moderate while larger donor-acceptor distances yield weak hydrogen bonds (Table S2, Supporting Information) existing between NH_4^+ ions and terminal and bridging oxygen atoms. Further hydrogen bonds can also be observed

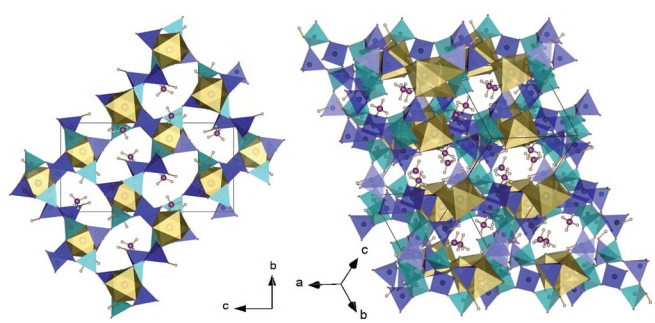

Figure 3. Oval shaped channels along [100] and [111]; yellow octahedra centered by manganese, blue, and turquoise tetrahedra centered by phosphorus and boron, respectively.

between the chlorine atom and the protonated borate (weak) and phosphate tetrahedra (moderate) as well as the NH_4^+ ions (weak).

To prove the phase purity of our sample, a Rietveld refinement based on the structure model of **I** was performed; this led to excellent residuals of R_p = 0.009, R_{wp} = 0.013 and χ^2 = 1.46 (Figure 4) and did not show any trace of other phases.

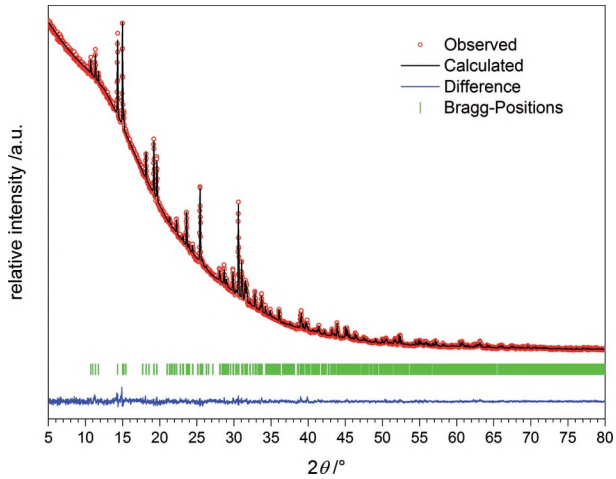

Figure 4. Xray diffraction pattern and result of the Rietveld refinement based on our structure model of $(NH_4)_2Mn[B_2P_3O_{11}(OH)_2]Cl$ obtained from single-crystal data; the high background originates from a relatively wide collimator to achieve a reasonable beam intensity.

Electrostatic Calculations

The coordination numbers of manganese and the electrostatic consistency of the structure model were proved by MAPLE calculations based on the MAPLE concept (*M*adelung *P*art of *L*attice *E*nergy).[47–49] A structure model is electrostatically consistent if the sum of MAPLE values of chemically similar compounds deviates from the MAPLE value of the compound of interest by less than approx. 1 %. According to our calculations, the structure model of $(NH_4)_2Mn[B_2P_3O_{11}(OH)_2]Cl$ thus shows electrostatic consistency, as presented in Table 2.

UV/Vis Spectroscopy

All excitations in a d^5 Mn^{2+} ion in an octahedral environment are spin and parity forbidden. Since the coordination environment of Mn^{2+} is slightly distorted those selection rules do not that strongly apply and two weak absorption bands can be observed in the UV/Vis reflection spectrum (Figure 5) at 360 ($^6S \rightarrow {}^4T_2$) and 405 nm ($^6S \rightarrow {}^4E$)[32,33] of $(NH_4)_2Mn[B_2P_3O_{11}(OH)_2]Cl$. Moreover, this spectrum is in agreement with the pink body-color of our sample.

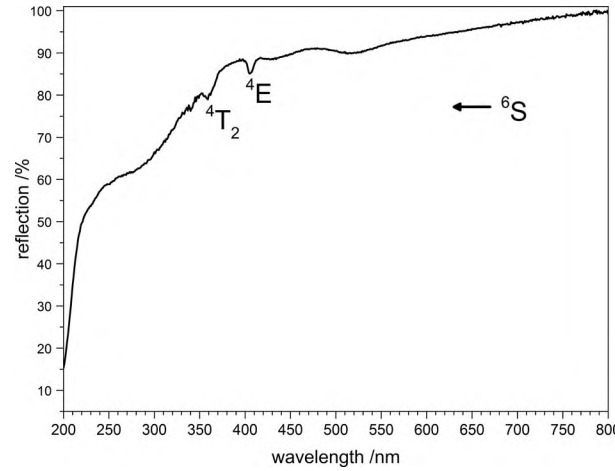

Figure 5. UV/Vis spectrum of $(NH_4)_2Mn[B_2P_3O_{11}(OH)_2]Cl$.

Infrared Spectroscopy

The infrared spectrum of **I** is shown in Figure 6. The bands at 3490, 3338, and 1666 cm^{-1} can be assigned to the stretching and deformation vibrations of the OH groups,[18,34–36] whereas vibrations between 3365–2617 cm^{-1} and at 1423 cm^{-1} can be assigned to N–H stretching vibrations.[37–39] Typical BO_4 vibrations can be found at 1163, 908, 887, 870, and 511 cm^{-1}, whereas typical PO_4 vibrations range in the relatively lower region between 1094 and 417 cm^{-1}, respectively. Characteristic bands of symmetric or asymmetric B–O–P stretching and bending vibrations are found at 830 (ν_{as}), 704 (ν_s), 606 (δ), and for δ(O–P–O) at 557 cm^{-1}.[40,41]

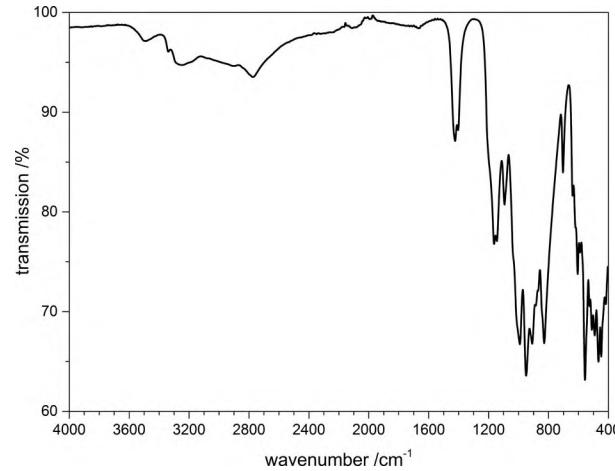

Figure 6. Infrared spectrum of $(NH_4)_2Mn[B_2P_3O_{11}(OH)_2]Cl$.

Magnetic Measurements

Since the crystal structure determination based on single-crystal data revealed the presence of several protons the valence state of manganese could only be postulated and in a first approach be confirmed by UV/Vis spectroscopy (see above). A real proof of the valence and spin state of manganese should

be delivered by a magnetic susceptibility measurement of $(NH_4)_2Mn[B_2P_3O_{11}(OH)_2]Cl$, recorded in the field of 1000 Oe over the temperature range of $1.8\ K < T < 400\ K$. In the whole temperature range the molar susceptibility obeys Curie's law ($\chi_m = C/T$) very well with a Curie constant of $C = 4.1897$ emu mol^{-1} K^{-1} (Figure 7). The Curie constant corresponds to an effective magnetic moment per Mn^{2+} ion of $\mu_{eff} = 5.79\ \mu_B$, which is close to the theoretical value of $\mu_{eff} = 5.92\ \mu_B$ and fits very well in the range of experimental effective magnetic moments of *high-spin* divalent Mn ions (5.65–6.10 μ_B).[42]

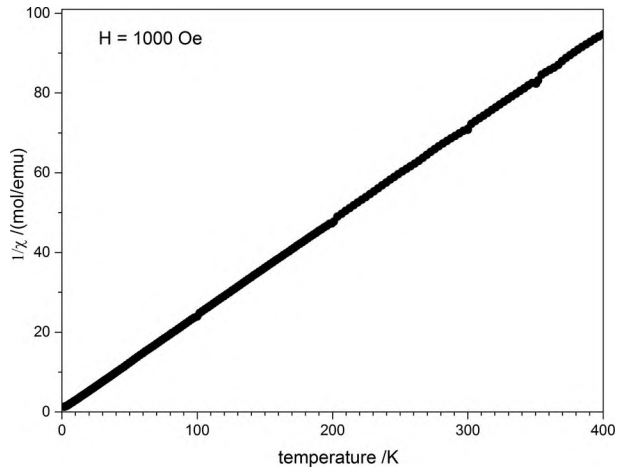

Figure 7. Temperature dependence of the inverse magnetic susceptibility of $(NH_4)_2Mn[B_2P_3O_{11}(OH)_2]Cl$.

Thermal Analysis

$(NH_4)_2Mn[B_2P_3O_{11}(OH)_2]Cl$ shows a reasonable stability against thermal treatment. The thermogravimetry curve (Figure 8) reveals a single step of mass loss of 21.1 wt% in the temperature range between 340 and 640 °C. Assuming that along with one mole of NH_4Cl a further mole of NH_3 and H_2O evaporates (theor. mass loss: 19.5 wt%) a composition of $Mn[B_2P_3O_{11}(OH)]$ might be expected. With further increasing temperature and maintaining the sample at 1350 °C a further mass loss of 2.6% is observed. X-ray powder diffraction analysis revealed $MnPO_4$ as crystalline product after the treatment at 1350 °C competing with an intense background. The latter might be due to amorphous B_2O_3 and P_2O_5, which show a strong tendency to become amorphous at higher temperatures. Heating the compound to 600 °C in a nitrogen atmosphere a crystalline intermediate was obtained. X-ray powder diffraction analysis revealed $Mn_2P_2O_7$ and BPO_4 as main and side product, respectively. Temperature-dependent X-ray powder diffraction confirms that **I** is stable up to 340 °C (Figure 9). At higher temperatures the formation of $Mn_2P_2O_7$ and BPO_4 is confirmed. It can be concluded that instead of forming $Mn[B_2P_3O_{11}(OH)]$ the borophosphate decomposes.

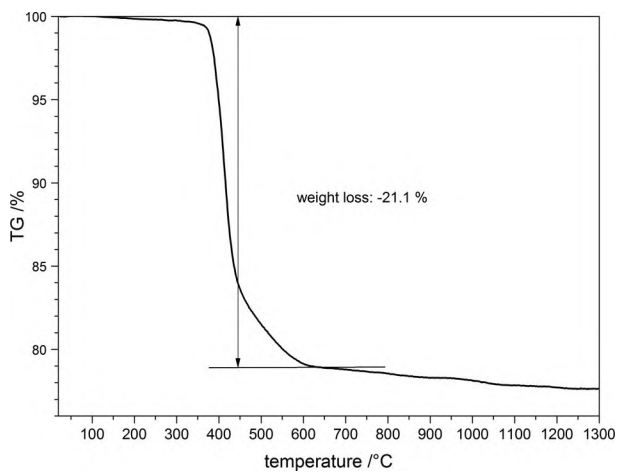

Figure 8. Thermogram of $(NH_4)_2Mn[B_2P_3O_{11}(OH)_2]Cl$.

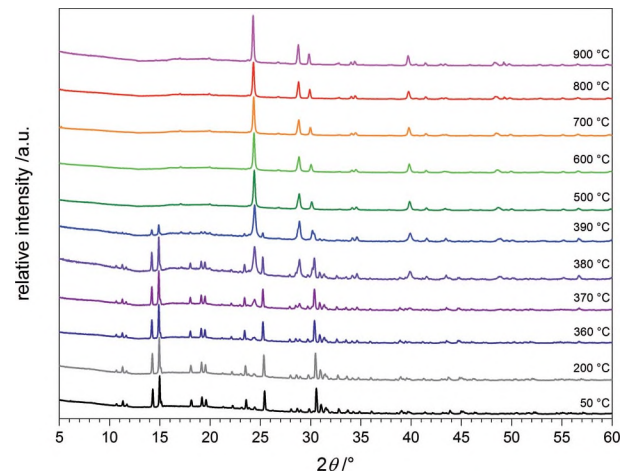

Figure 9. Temperature-dependent X-ray diffraction patterns of $(NH_4)_2Mn[B_2P_3O_{11}(OH)_2]Cl$ recorded between 50–900 °C.

Conclusions

In this contribution we demonstrated the phase-pure synthesis, crystal structure determination, and spectroscopic characterization of $(NH_4)_2Mn[B_2P_3O_{11}(OH)_2]Cl$ as a new representative of the borophosphate family. The oB vierer-single ring $^2_\infty[B_2P_3\Phi_{13}]$ (Φ = O, OH) as a novel FBU forms lB vierer-single layers with NH^{4+}, Mn^{2+}, and Cl^- ions in-between. All observed bands in the IR spectrum could be assigned to the corresponding groups. The compound shows weak absorption in the visible range as possible transitions are parity and spin forbidden and thus appears colorless. Two weak absorption bands in the UV region are still visible because the coordination sphere of Mn^{2+} is distorted octahedrally. The valence and spin state of the manganese ions are further confirmed by the magnetic measurements revealing the oxidation state of Mn^{II} and thus the composition of the title compound; moreover, no interaction between the Mn^{2+} atoms could be detected. The two layered structure is stable up to 340 °C before presumably NH_4Cl, NH_3, and H_2O are released to form $Mn_2P_2O_7$ and BPO_4 and further amorphous compounds.

Experimental Section

Syntheses: $(NH_4)_2Mn[B_2P_3O_{11}(OH)_2]Cl$ was synthesized under hydrothermal conditions. A mixture of $MnCl_2$ (251.5 mg, 2.014 mmol, Fluka, 99 %), $(NH_4)_2HPO_4$ (528.4 mg, 4.002 mmol, Merck, 99 %), H_3BO_3 (123.7 mg, 2.053 mmol, Merck, 99.8 %), and H_3PO_4 (0.4 mL, VWR 85 %) was transferred into a 10 mL Teflon autoclave and was kept at 180 °C; after 8 d a slightly pink suspension was obtained. The product was washed with hot water, filtered off, and dried in air overnight. $(NH_4)_2Mn[B_2P_3O_{11}(OH)_2]Cl$ was obtained as an almost colorless, crystalline powder.

X-ray Powder Diffraction: The crystalline sample was finely ground, enclosed in a Hilgenberg glass capillary of 0.3 mm outer diameter and investigated at room temperature with a Bruker D8 Advance diffractometer using Cu-K_α radiation (LynxEye 1-D detector, steps of 0.2°, acquisition time 7 s per step, soller slits 2.5°, fixed divergence slit 8 mm, transmission geometry), the obtained product was phase pure according to X-ray powder diffractometry. The structure model was confirmed and refined by Rietveld analysis[43,44] (Figure 4) using the FullProf program suite and the WINPlotR graphical user interface.[45]

For the temperature-dependent measurement (Figure 9) the sample was enclosed in a silica-glass Hilgenberg capillary of 0.5 mm outer diameter and treated between 50 and 900 °C on the same instrument. The generator was driven at 40 kV and 40 mA.

Crystal Structure Analyses: A suited single-crystal was selected for single-crystal X-ray diffraction analysis under a polarizing microscope. Diffraction data were collected with a Bruker D8 Venture diffractometer using Mo-K_α radiation (λ = 0.7093 Å) at a temperature of 297 ± 2 K. The structure was solved by direct methods and refined by full-matrix least-squares technique with the SHELXTL crystallographic software package.[46] The Mn, B, P, O, and Cl atoms could be clearly located and the N atoms were subsequently assigned from the difference Fourier map. Hydrogen atoms were added geometrically and were confirmed by MAPLE calculations.[47–49] Relevant crystallographic data and further details of the structure determination are summarized in Table 3. Table 4 and Table S1 (Supporting Information) show positional and displacement parameters for all atoms, respectively.

Further details of the crystal structure investigations may be obtained from the Fachinformationszentrum Karlsruhe, 76344 Eggenstein-Leopoldshafen, Germany (Fax: +49-7247-808-666; E-Mail: crysdata@fiz-karlsruhe.de, http://www.fiz-karlsruhe.de/request for deposited data.html) on quoting the depository number CSD-429214 for $(NH_4)_2Mn[B_2P_3O_{11}(OH)_2]Cl$.

Infrared Spectroscopy: An infrared spectrum was recorded at room temperature with a Bruker EQUINOX 55 FT-IR spectrometer using a Platinum ATR device with a scanning range from 4000 to 400 cm^{-1}.

UV/Vis Spectroscopy: The optical reflection spectrum of $(NH_4)_2Mn[B_2P_3O_{11}(OH)_2]Cl$ was recorded with a Varian Cary 300 Scan UV/Vis spectrophotometer in the range of 200–800 nm.

Magnetic Investigations: The temperature-dependent magnetic susceptibility data were recorded with a Quantum Design MPMS-XL super-conducting quantum-interference device (SQUID) magnetometer in the field of 1000 Oe between 1.8 K < T < 400 K; the data are shown in Figure 7 and Figure S1 (Supporting Information).

Table 3. Crystal data and structure refinements.

	$(NH_4)_2Mn[B_2P_3O_{11}(OH)_2]Cl$ (**I**)
Temperature /K	297(2)
Molar weight /g·mol^{-1}	450.87
Crystal system	monoclinic
Space group	$P2_1/n$ (no. 14)
a /pm	905.24(3)
b /pm	847.29(3)
c /pm	1652.32(5)
β /°	92.303(1)
V /10^6 pm^3	1266.31(7)
Z	4
Calculated density ρ_x /g·cm^{-3}	2.366
Color	colorless
Dimensions /mm^3	0.044 × 0.034 × 0.026
μ /mm^{-1}	1.709
F(000)	900
Radiation	Mo-K_α (λ = 0.7093 Å)
Diffractometer	Bruker D8 Venture
Absorption correction	multi-scan
Index range (hkl)	–10/–10/–19–9/10/19
Theta range (θ_{min}–θ_{max}) /°	2.47–25.00
Reflections collected	33345
Independent reflections	2227
Parameters	229
R_{int}	0.033
R_1(all data)	0.025
wR_2(all data)	0.063
Goodness of fit (GooF)	1.057
Residual electron density, min/max /e·10^{-6} pm^{-3}	–0.39/ 0.38
Rietveld refinement:	
a /pm	905.29(2)
b /pm	846.69(2)
c /pm	1651.65(3)
β /°	92.272(1)
V /10^6 pm^3	1264.99(4)
R_p, R_{wp}, χ^2	0.009 / 0.013 / 1.46

Thermal Analysis: Thermal analysis was carried out with a Netzsch STA-409 PC thermal analyzer in the temperature range of 22–1350 °C in a nitrogen atmosphere with a heating rate of 5 °C·min^{-1}.

Supporting Information (see footnote on the first page of this article): Plot of the temperature dependence of the magnetic susceptibility; anisotropic displacement parameters and hydrogen bonding parameters of $(NH_4)_2Mn[B_2P_3O_{11}(OH)_2]Cl$.

Acknowledgements

The authors thank *Dana Vieweg*, Universität Augsburg, for recording the magnetic susceptibility measurements and *Dr. Stefan Riegg*, Universität Augsburg, for valuable discussions about the magnetic measurement and the Rietveld refinement.

References

[1] R. Kniep, G. Gözel, B. Eisenmann, C. Röhr, M. Asbrand, M. Kizilyalli, *Angew. Chem. Int. Ed. Engl.* **1994**, *33*, 749–751.
[2] R. P. Bontchev, S. C. Sevov, *Inorg. Chem.* **1996**, *35*, 6910–6911.
[3] C. Hauf, R. Kniep, *Z. Kristallogr. NCS* **1996**, *211*, 705–706.
[4] C. Hauf, R. Kniep, *Z. Kristallogr.* **1996**, *211*, 707–708.
[5] S. C. Sevov, *Angew. Chem.* **1996**, *108*, 2814–2816.
[6] R. Kniep, H. G. Will, I. Boy, C. Röhr, *Angew. Chem. Int. Ed. Engl.* **1997**, *36*, 1013–1014.

Table 4. Atomic coordinates, Wyckoff symbols, and isotropic displacement parameters U_{eq} /Å^2 in $(NH_4)_2Mn[B_2P_3O_{11}(OH)_2]Cl$ (O_{br} = bridging oxygen atom; O_{term} = terminal oxygen atom; O_H = oxygen atom of hydroxyl group).

Atom	Wyckoff symbol	*x*	*y*	*z*	U_{eq}
Mn1	4*e*	0.59947(4)	0.32262(4)	0.12898(2)	0.01166(11)
P1	4*e*	0.29996(6)	0.42566(7)	0.01813(3)	0.00949(14)
P2	4*e*	0.83510(6)	0.04260(7)	0.06081(3)	0.01068(14)
P3	4*e*	0.27023(6)	0.23250(7)	0.20832(3)	0.00939(14)
B1	4*e*	0.3347(3)	0.5426(3)	0.17167(14)	0.0104(5)
B2	4*e*	0.1164(3)	0.1762(3)	0.06228(15)	0.0119(5)
$O_{br}1$	4*e*	0.21770(17)	0.19090(18)	0.29369(8)	0.0121(3)
$O_{br}2$	4*e*	0.30031(17)	0.55873(18)	0.08407(9)	0.0134(3)
$O_{br}3$	4*e*	0.15300(16)	0.33059(18)	0.03033(9)	0.0134(3)
$O_{br}4$	4*e*	0.81070(18)	–0.0463(2)	–0.02000(9)	0.0139(4)
$O_{br}5$	4*e*	0.95483(17)	0.16715(19)	0.05047(10)	0.0175(4)
$O_{br}6$	4*e*	0.15745(18)	0.15515(19)	0.14816(9)	0.0173(4)
$O_{br}7$	4*e*	0.24534(16)	0.41298(18)	0.20465(9)	0.0121(3)
$O_{term}1$	4*e*	0.43173(17)	0.31920(18)	0.03093(9)	0.0151(3)
$O_{term}2$	4*e*	0.28264(17)	0.50379(19)	–0.06327(8)	0.0148(3)
$O_{term}3$	4*e*	0.69029(17)	0.11352(19)	0.08056(10)	0.0165(3)
$O_{term}4$	4*e*	0.42656(17)	0.18467(19)	0.19612(9)	0.0165(4)
O_H1	4*e*	0.48994(17)	0.5182(2)	0.18745(9)	0.0168(4)
O_H2	4*e*	0.89442(19)	–0.0782(2)	0.12516(10)	0.0231(4)
Cl1	4*e*	0.79760(7)	0.30866(8)	0.24497(3)	0.02532(16)
N1	4*e*	0.0242(2)	0.4200(3)	–0.14034(13)	0.0236(5)
N2	4*e*	0.4566(3)	–0.1180(3)	0.09562(13)	0.0241(5)
H1	4*e*	0.548(3)	0.585(3)	0.2234(16)	0.050
H2	4*e*	0.835(3)	–0.102(4)	0.1709(14)	0.050
H3	4*e*	–0.043(3)	0.502(3)	–0.1260(19)	0.050
H4	4*e*	–0.007(4)	0.321(2)	–0.1178(19)	0.050
H5	4*e*	0.1203(19)	0.448(4)	–0.1165(18)	0.050
H6	4*e*	0.017(4)	0.396(4)	–0.1974(8)	0.050
H7	4*e*	0.366(2)	–0.069(4)	0.0751(19)	0.050
H8	4*e*	0.526(3)	–0.033(3)	0.103(2)	0.050
H9	4*e*	0.498(4)	–0.192(3)	0.0581(16)	0.050
H10	4*e*	0.457(4)	–0.166(4)	0.1484(10)	0.050

[7] R. Kniep, H. Engelhardt, *Z. Anorg. Allg. Chem.* **1998**, *624*, 1291–1297.
[8] R. Kniep, H. Engelhardt, C. Hauf, *Chem. Mater.* **1998**, *10*, 2930–2934.
[9] Y. Shi, J. Liang, H. Zhang, Q. Liu, X. Chen, J. Yang, W. Zhuang, G. Rao, *J. Solid State Chem.* **1998**, *135*, 43–51.
[10] R. Kniep, G. Schäfer, H. Engelhardt, I. Boy, *Angew. Chem. Int. Ed.* **1999**, *38*, 3641–3644.
[11] F. Liebau, *Structural Chemistry of Silicates*, Springer-Verlag, Berlin Heidelberg **1985**.
[12] B. Ewald, Y.-X. Huang, R. Kniep, *Z. Anorg. Allg. Chem.* **2007**, *633*, 1517–1540.
[13] W. Loewenstein, M. Loewenstein, *Am. Mineral.* **1954**, *39*, 92–96.
[14] L. Pauling, *J. Am. Chem. Soc.* **1929**, *51*, 1010–1026.
[15] P. C. Burns, J. D. Grice, F. C. Hawthorne, *Can. Mineral.* **1995**, *33*, 1131–1151.
[16] J. D. Grice, P. C. Burns, F. C. Hawthorne, *Can. Mineral.* **1999**, *37*, 731–762.
[17] H. Engelhardt, W. Schnelle, R. Kniep, *Z. Anorg. Allg. Chem.* **2000**, *626*, 1380–1386.
[18] G.-Y. Yang, S. C. Sevov, *Inorg. Chem.* **2001**, *40*, 2214–2215.
[19] W. Liu, M. X. Yang, H. Chen, M. Li, J. Zhao, *Inorg. Chem.* **2004**, *43*, 3910–3914.
[20] B. Ewald, Y. Prots, P. Menezes, S. Natarajan, H. Zhang, R. Kniep, *Inorg. Chem.* **2005**, *44*, 6431–6438.
[21] Y.-X. Huang, O. Hochrein, D. Zahn, Y. Prots, H. Borrmann, R. Kniep, *Chem. Eur. J.* **2007**, *13*, 1737–1745.
[22] T. Balić-Žunić, E. Makovicky, *Acta Crystallogr., Sect. B* **1996**, *52*, 78–81.
[23] E. Makovicky, T. Balić-Žunić, *Acta Crystallogr., Sect. B* **1998**, *54*, 766–773.
[24] H. A. Höppe, M. Daub, O. Oeckler, *Solid State Sci.* **2009**, *11*, 1484–1488.
[25] R. D. Shannon, *Acta Crystallogr., Sect. A* **1976**, *32*, 751–767.
[26] T. Steiner, *Angew. Chem. Int. Ed.* **2002**, *41*, 48–76.
[27] S. Sasaki, K. Fujino, Y. Takeuchi, *Proc. Jpn. Acad. Ser. B* **1979**, *55*, 43–48.
[28] G. E. Gurr, P. W. Montgomery, C. D. Knutson, B. T. Gorres, *Acta Crystallogr., Sect. B* **1970**, *26*, 906–915.
[29] K. Mansikka, J. Poyhonen, *Ann. Acad. Sci. Fenn. Ser. A* **1962**, *6*, 118–118.
[30] A. A. Khan, W. H. Baur, *Acta Crystallogr., Sect. B* **1973**, *29*, 2721–2726.
[31] C. H. MacGillavry, H. C. J. de Decker, L. M. Nijland, *Nature* **1949**, *164*, 448–449.
[32] G. Wang, M. Valldor, C. Lorbeer, A.-V. Mudring, *Eur. J. Inorg. Chem.* **2012**, 3032–3038.
[33] L. E. Orgel, *J. Chem. Phys.* **1955**, *23*, 1824–1826.
[34] A. Yilmaz, L. Tatar Yıldırım, X. Bu, M. Kizilyalli, G. D. Stucky, *Cryst. Res. Technol.* **2005**, *40*, 579–585.
[35] Y.-X. Huang, B. Ewald, W. Schnelle, Y. Prots, R. Kniep, *Inorg. Chem.* **2006**, *45*, 7578–7580.
[36] T. Yang, J. Ju, F. Liao, J. Sasaki, N. Toyota, J. Lin, *J. Solid State Chem.* **2008**, *181*, 1110–1115.
[37] Y.-X. Huang, G. Schäfer, W. Carrillo-Cabrera, R. Cardoso, W. Schnelle, J.-T. Zhao, R. Kniep, *Chem. Mater.* **2001**, *13*, 4348–4354.
[38] W. Yang, J. Li, T. Na, J. Xu, L. Wang, J. Yu, R. Xu, *Dalton Trans.* **2011**, *40*, 2549–2554.
[39] H. Shi, Y. Feng, Q. Huang, D. Qiu, M. Li, K. Liu, *CrystEngComm* **2011**, *13*, 7185–7188.

[40] A. Baykal, M. Kizilyalli, R. Kniep, *J. Mater. Sci.* **2000**, *35*, 4621–4626.
[41] A. Baykal, G. Gözel, M. Kizilyalli, R. Kniep, *Turk. J. Chem.* **2000**, *24*, 381–388.
[42] H. Lueken, *Magnetochemie*, B. G. Teubner Stuttgart, **1999**.
[43] H. Rietveld, *J. Appl. Crystallogr.* **1969**, *2*, 65–71.
[44] H. M. Rietveld, *Z. Kristallogr.* **2010**, *225*, 545–547.
[45] J. Rodríguez-Carvajal, *J. Phys. Condens. Matter* **1993**, *192*, 55–69.
[46] G. M. Sheldrick, *Acta Crystallogr., Sect. A* **2008**, *64*, 112–122.
[47] R. Hoppe, *Angew. Chem. Int. Ed. Engl.* **1966**, *5*, 95–106.
[48] R. Hoppe, *Angew. Chem. Int. Ed. Engl.* **1970**, *9*, 25–34.
[49] R. Hübenthal, *MAPLE*, Program for the Calculation of the Madelung Part of Lattice Energy, University of Gießen, Germany, **1993**.